Interatrial distance predicts the necessity of additional carina ablation to isolate the right-sided pulmonary veins

Yuichi Hanaki, MD,*† Kentaro Yoshida, MD,*† Masako Baba, MD,*† Hideyuki Hasebe, MD,† Noriyuki Takeyasu, MD,* Akihiko Nogami, MD,† Masaki Ieda, MD†

*From the *Department of Cardiology, Ibaraki Prefectural Central Hospital, Kasama, Japan, and †Department of Cardiology, Faculty of Medicine, University of Tsukuba, Tsukuba, Japan.*

BACKGROUND Ablation of the pulmonary vein (PV) carina is occasionally required for PV isolation (PVI). Marshall bundle and epicardial connections between the right-sided PV (RtPV) carina and right atrium (RA) may be one of the mechanisms that necessitates carina ablation.

OBJECTIVE We sought to clarify anatomical characteristics predictive of the necessity of carina ablation.

METHODS Forty-five consecutive patients undergoing radiofrequency catheter ablation of atrial fibrillation were prospectively included in this study. Left atrial (LA) and PV size and morphology, and interatrial distance in the posterior aspect, were measured on cardiac computed tomography (CT) images.

RESULTS For right-sided PVI, the patients were divided into 2 groups based on the necessity of RtPV carina ablation, Carina-ABL group (n = 21) and Non-Carina-ABL group (n = 24). The distance between the anterior portion of the RtPV carina and RA was shorter in the Carina-ABL group vs in the Non-Carina-ABL group (7.7 ± 1.7 mm/m^2 vs 9.5 ± 2.3 mm/m^2; $P = .005$), whereas other anatomical parameters (LA and RA volumes, right inferior PV angle, and ostial diameters of the RtPVs) did not differ between the groups. For left-sided PVI, the ostial diameter and circumference of the left superior PV were smaller in the Carina-ABL group (n = 13) vs the Non-Carina-ABL group (n = 32) (8.6 ± 2.1 mm/m^2 vs 7.3 ± 1.5 mm/m^2; $P = .044$, and 34.9 ± 6.0 mm/m^2 vs 30.1 ± 5.1 mm/m^2; $P = .017$, respectively).

CONCLUSIONS A shorter interatrial distance for right-sided PVI and a smaller PV ostium for left-sided PVI were associated with the necessity of additional carina ablation. The presence and location of the epicardial fibers may be affected by the atrial and PV geometry.

KEYWORDS Ablation; Atrial fibrillation; Carina; Epicardial connection; Pulmonary vein

(Heart Rhythm O^2 2020;1:259–267)

Introduction

Pulmonary vein (PV) isolation (PVI) is a standard strategy determined as a class I recommendation for catheter ablation of atrial fibrillation (AF).[1] Although technological advancements such as 3-dimensional (3-D) mapping, irrigation-tip catheters, contact-force monitoring, and an algorithm estimating radiofrequency lesion size[2] have improved the efficacy and safety of the procedures, electrical isolation of the PVs is occasionally difficult to achieve without additional ablation at the carina region, especially in the right-sided PVs. A few prior studies have suggested the presence of a Marshall bundle and an epicardial connection between the carina region and right atrium (RA) as one of the mechanisms that necessitates carina ablation.[3–8]

Recently, we added a novel electrophysiological analysis advancing this suggestion and interpretation. In patients undergoing catheter ablation of AF, the presence of a conduction breakthrough at the carina region during sinus rhythm highly predicted the necessity of performing additional carina ablation to isolate the right-sided PVs.[5,7,8] In the present study, we hypothesized that anatomical and morphological characteristics of the left atrium (LA), RA, and PVs, and their interrelation may determine where the terminal site of an epicardial bridging fiber attaches and may affect the associated results of catheter ablation, such as an occurrence of carina breakthrough during sinus rhythm and the necessity of additional carina ablation.

Address reprint requests and correspondence: Dr Kentaro Yoshida, Department of Cardiology, Faculty of Medicine, University of Tsukuba, 1-1-1 Tennodai, Tsukuba 305-8575, Japan. E-mail address: kenyoshi@md.tsukuba.ac.jp.

2666-5018/

https://doi.org/10.1016/j.hroo.2020.08.003

KEY FINDINGS

- A Marshall bundle and an epicardial connection between the right-sided pulmonary venous (PV) carina and right atrium may be one of the mechanisms for which carinal ablation is required for PV isolation (PVI).
- A shorter interatrial distance for right-sided PVI and a smaller PV ostium for left-sided PVI are associated with the necessity of additional carina ablation.
- The presence and location of the epicardial fibers may be affected by the atrial and PV geometry.

Methods

Study subjects

Forty-five consecutive patients referred to Ibaraki Prefectural Central Hospital for initial catheter ablation of AF from April 2019 to November 2019 were prospectively included in this study. Patients with long-standing persistent AF and/or structural heart disease were excluded from the study. All antiarrhythmic drug therapy was discontinued 4–5 half-lives before the procedure, except for amiodarone, which was discontinued 8 weeks beforehand. The study protocol was approved by the hospital's institutional review board and complied with the Declaration of Helsinki. Written informed consent was obtained from all patients.

Electrophysiological study and catheter ablation

Electrophysiological study and catheter ablation proceeded under conscious sedation with dexmedetomidine and fentanyl. Surface electrocardiograms and intracardiac electrograms were continuously monitored and stored on an EP-WorkMate recording system (Abbott, Saint Paul, MN). A 6F 20-pole dual-site mapping catheter (BeeAT; Japan Lifeline Co, Ltd, Tokyo, Japan) was inserted through the subclavian vein and positioned in the coronary sinus, RA, and superior vena cava (SVC) throughout the procedure. An intracardiac echocardiography catheter (AcuNav; Biosense Webster, Diamond Bar, CA) was advanced to the RA via the femoral approach to guide transseptal puncture. Two long sheaths (SL0; AF Division, Abbott) were then advanced into the LA. If the patients presented to the laboratory in AF, internal cardioversion using a BeeAT catheter was performed. If it was difficult to maintain sinus rhythm after the cardioversion, such patients were excluded from the study. During sinus rhythm, each PV and the LA, SVC, and RA were mapped with a duodecapolar mapping catheter (PENTARAY; Biosense Webster). Points were acquired using the CARTO ConfiDENSE module (Biosense Webster) in the auto-freeze mode.[9]

After obtaining activation maps of the LA and RA including SVC (mean number of mapping points: 1544 ± 677 and 717 ± 434, respectively), electrograms recorded at the left-sided septum were carefully reviewed by K.Y., who was blinded to the information from cardiac computed tomography (CT) imaging, and far-field electrograms from the SVC and RA were manually removed. Near-field or far-field electrograms were discriminated by using their morphologies (sharp or dull) and near-field SVC potentials directly and simultaneously recorded by the BeeAT catheter. Carina breakthrough was determined based on a centrifugal activation pattern depicted at the inter-PV carina inside the planned ablation line, which was designed by the operator (Y.H.), who was blinded to the presence or absence of carina breakthrough.

The ipsilateral PV antrum was circumferentially ablated with a ThermoCool STSF catheter under CARTO guidance (Biosense Webster) using real-time automated display of radiofrequency applications (Visitag; Biosense Webster). Radiofrequency energy was delivered at a power of 20–25 W at the posterior aspect, at 15–20 W at the sites adjacent to the esophagus, and at 25–35 W at the anterior aspect of the PV antrum. Target values of the ablation index (Biosense Webster) were 450 for the anterior aspect and 350 for the posterior aspect of the PV antrum, and the targeted interlesion distance was 4 mm. PVI with entrance and exit blocks was confirmed with the Lasso catheter (Biosense Webster, Irvine, CA) and a pacing maneuver performed within the isolation line with an ablation catheter (Non-Carina-ABL group). If PVI was not achieved by circumferential ablation at the antral level, careful remapping to identify gaps with the Lasso and ThermoCool catheters and additional ablation at the same power setting on the initial ablation line was repeated to achieve elimination of residual potentials. If PVI was not achieved even after remapping and reablation at the antral level, earliest activation sites at the PV carina were ablated. If this carina ablation resulted in successful PVI, this patient was classified into the Carina-ABL group.

Cardiac computed tomography

CT examinations were performed within 7 days before the ablation procedure with a 320-row CT scanner (Somatom Definition Flash; Siemens AG, Erlangen, Germany). The parameters for CT imaging were prospective electrocardiogram-gated acquisitions; tube potential, 120 kVp; and detector configuration, 320 × 0.5 mm. A volume of 1.5 mL/kg of contrast was injected at an injection rate of 7.0 mL/s. Scanning was initiated after a threshold of 150 Hounsfield units was reached in the ascending aorta during expiratory breath holding. The CT images were reconstructed at a 0.5-mm slice thickness in the diastolic phase (basically 75%–77%) of the R-R interval. Data reconstruction and the measurements of LA and RA volumes were performed on a postprocessing workstation with the use of 2-dimensional viewing modes (SYNAPSE VINCENT; FUJIFILM, Tokyo, Japan). The LA, RA, and PVs were reconstructed with 3-D segmentation software using a CARTO 3 system (Biosense Webster). A physician (M.B.) blinded to the study aim, concept, and ablation results measured the following

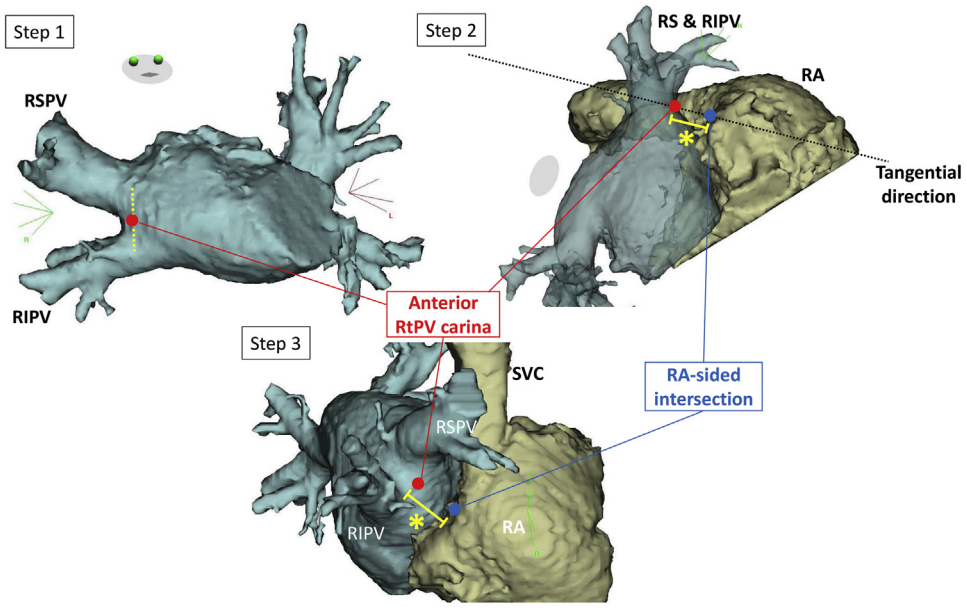

Figure 1 Protocol for the measurements of interatrial distance. See text for details. LIPV = left inferior pulmonary vein; LSPV = left superior PV; RA = right atrium; RIPV = right inferior PV; RtPV = right-sided PV; RSPV = right superior PV; SVC = superior vena cava.

parameters in 3 different orthogonal planes (transverse, sagittal, and coronal views) with multiplanar reformatting function:

(1) LA and RA volumes (mL/m^2). These were calculated using the biplane method with multiplanar reformatting function.[10]
(2) The number of PVs.
(3) Minor- and major-axis diameters of each PV ostium (mm/m^2).[11,12]
(4) Circumferences at the ostium level (mm/m^2).[11,12]
(5) Cross-sectional area.[13,14] This was calculated according to the following formula: $\pi \times$ (major axis / 2) $\times$ (minor axis / 2).
(6) PV ostial morphology, defined as a *flattening rate* using the ratio of the minor-axis diameter divided by major-axis diameter.[12]
(7) Right inferior PV (RIPV) angle (branching angle of the RIPV to the coronal plane).[15] The RIPV angle was defined as the angle between the line that runs longitudinally in the center of the RIPV and coronal plane in horizontal CT imaging, in which the ostium of the RIPV is rendered, to estimate the extent of the posterior direction of the RIPV.
(8) Interatrial distance in the posterior aspect (mm/m^2). This was determined by the following protocols, as shown in Figure 1:
    (i) The ostia of the right superior PV and RIPV were determined by the method described above.
    (ii) A common tangent of the PV ostia was drawn (anterior tangent).
    (iii) A mid-point of the anterior tangent between the right superior PV and RIPV was determined.
    (iv) The map was rotated to the inferosuperior view, as shown in step 2 of Figure 1, and its transmissivity was decreased to <30% to visualize the mid-carina area tangentially.
    (v) A tangent of the right-sided PV antrum, which also crosses at right angles to the mid-point of the anterior tangent, was drawn, and its landing point on the RA was determined.
    (vi) Finally, interatrial distance was defined as the distance between the mid-point of the anterior tangent and the landing point on the RA.

Ten patients were selected at random for the assessments of the intraobserver and interobserver reproducibilities by M.B. and H.H.

Statistical analysis

Continuous variables are expressed as mean ± standard deviation (SD) or median [25th–75th percentile], and categorical variables are reported as number and percentage. Differences between groups were tested using the unpaired Student *t* test, Mann-Whitney *U* test, χ^2 analysis, or Fisher test as appropriate. Also, a univariate logistic regression analysis was performed to reveal factors associated with the necessity of carina ablation. A 2-tailed *P* value of <.05 indicated statistical significance. All statistical analyses were carried out using JMP version 12.0 (SAS Institute Inc, Cary, NC).

Results

Patient characteristics

Patient characteristics are presented in Table 1. All PVs were successfully isolated. No major complications such as stroke, cardiac tamponade, or atrial-esophageal fistula occurred.

Table 1 Baseline clinical characteristics (right-sided pulmonary vein isolation)

Characteristic	Total (n = 45)	Carina ABL (n = 21)	Non-Carina ABL (n = 24)	*P*
Age, years	62.6 ± 8.6	61.4 ± 7.9	63.7 ± 9.2	.369
Male sex, n (%)	31 (68.9%)	14 (66.7%)	17 (70.8%)	.763
Body surface area, m^2	1.81 ± 0.21	1.83 ± 0.19	1.79 ± 0.22	.451
Body mass index, kg/m^2	25.4 ± 3.1	26.1 ± 3.1	24.8 ± 3.0	.146
Duration of AF history, months	13 [6, 26]	18 [7.5, 35]	12.5 [5.75, 24.0]	.312
$CHADS_2$ score	1.0 [0.0, 2.0]	1.0 [0.0, 2.0]	1.0 [0.0, 2.75]	.438
Persistent AF, n (%)	16 (35.6%)	6 (28.6%)	10 (41.7%)	.360
Hypertension, n (%)	24 (53.3%)	11 (52.4%)	13 (54.2%)	.905
Diabetes mellitus, n (%)	8 (17.8%)	4 (19.0%)	4 (16.7%)	.569
Ischemic heart disease, n (%)	3 (6.7%)	1 (4.8%)	2 (8.3%)	.551
Sick sinus syndrome, n (%)	3 (6.7%)	1 (4.8%)	2 (8.3%)	.551
History of stroke or TIA, n (%)	6 (13.3%)	2 (9.5%)	4 (16.7%)	.400
eGFR, $mL/min/1.73\ m^2$	65.8 ± 11.1	67.3 ± 12.9	64.6 ± 9.3	.418
BNP, pg/mL	27.4 [15.3, 53.8]	24.4 [13.8, 52.3]	37.4 [15.3, 165.6]	.498
Treatment before the procedure				
Class I AADs, n (%)	12 (26.7%)	4 (19.0%)	8 (33.3%)	.280
Amiodarone, n (%)	9 (20.0%)	3 (14.3%)	6 (25.0%)	.303
Bepridil, n (%)	3 (6.7%)	1 (4.8%)	2 (8.3%)	.551
Echocardiography				
LV end-diastolic diameter, mm	47.8 ± 5.5	48.2 ± 6.1	47.4 ± 5.0	.636
LV end-systolic diameter, mm	31.8 ± 6.5	32.0 ± 6.3	31.5 ± 6.8	.816
LV ejection fraction, %	60.9 ± 11.2	63.2 ± 6.5	59.3 ± 13.5	.313
LA volume index, mm/m^2	31.7 ± 10.5	30.0 ± 9.3	33.2 ± 11.5	.361

Results are shown as mean ± SD, median [interquartile range], or n (%).

AAD = antiarrhythmic drugs; ABL = ablation; AF = atrial fibrillation; BNP = B-type natriuretic peptide; eGFR = estimated glomerular filtration rate; LA = left atrium; LV = left ventricular; PV = pulmonary vein; TIA = transient ischemic attack.

Right-sided PV isolation

Relation between carina breakthrough and carina ablation

The LA activation maps revealed the carina breakthrough in addition to the Bachmann bundle breakthrough in 23 (51%) and Bachmann bundle breakthrough alone in 22 (49%) patients. Twenty-four (53%) patients were classified into the Non-Carina-ABL group, and 21 (47%) were classified into the Carina-ABL group. Nineteen (90.5%) patients had a carina breakthrough in the Carina-ABL group, whereas only 4 patients (16.7%) had a carina breakthrough in the Non-Carina-ABL group ($P < .001$) (Figure 2A).

Catheter ablation

Both procedure time (236 ± 35 minutes vs 200 ± 33 minutes, $P = .001$) and radiofrequency ablation time (51.0 ± 9.4 minutes vs 40.9 ± 8.6 minutes, $P = .001$) were longer in the Carina-ABL group vs in the Non-Carina-ABL group, whereas the length of the ablation line encircling the right-sided PVs and the encircled area (cross-sectional area isolated) were similar between the groups (11.8 ± 1.8 cm vs 12.3 ± 1.9 cm, $P = .52$, and 18.7 ± 4.4 cm^2 vs 22.8 ± 14.9 cm^2, $P = .2$) (Table 2). Also, the distance between the anterior encircling line and PV ostia was comparable between the groups (8.8 ± 2.0 mm/m^2 vs 8.8 ± 2.3

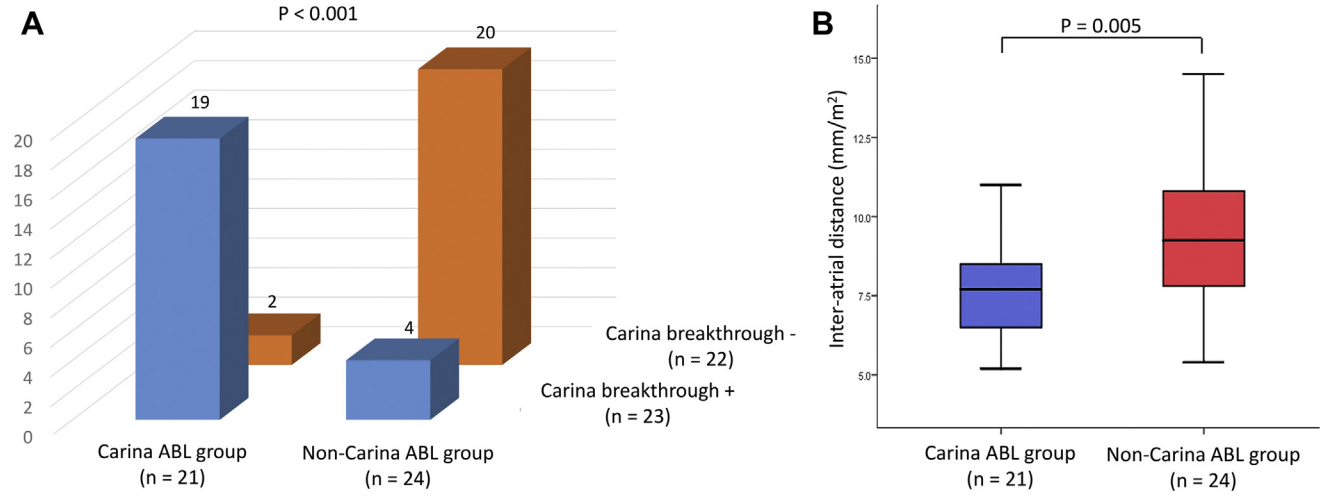

Figure 2 **A:** Relation between carina breakthrough and right-sided pulmonary vein carina ablation. **B:** Interatrial distance indexed to body surface area in the Carina-ABL and Non-Carina-ABL groups. ABL = ablation.

Table 2 Computed tomography measurements (right-sided pulmonary vein isolation)

	Total (n = 45)	Carina ABL (n = 21)	Non-Carina ABL (n = 24)	*P*
LA volume index, mL/m^2	37.7 ± 24.4	35.5 ± 18.7	39.9 ± 29.1	.562
RA volume index, mL/m^2	31.1 ± 11.6	29.7 ± 12.0	32.5 ± 11.3	.433
LA/RA ratio	0.91 ± 0.27	0.89 ± 0.24	0.94 ± 0.29	.575
Right middle PV	8 [17.8%]	3 [14.3%]	5 [20.8%]	.431
Right superior PV anatomy				
Major-axis diameter, mm/m^2	12.2 ± 2.4	12.2 ± 2.6	12.3 ± 2.2	.874
Minor-axis diameter, mm/m^2	9.2 ± 2.1	8.7 ± 2.1	9.6 ± 2.1	.171
Ostial morphology	0.76 ± 0.16	0.73 ± 0.17	0.79 ± 0.14	.224
Ostial circumference, mm/m^2	37.6 ± 7.6	36.2 ± 7.3	38.8 ± 7.8	.251
Cross-sectional area, mm^2/m^2	160.0 ± 50.8	153.7 ± 53.2	165.2 ± 49.1	.454
Right inferior PV anatomy				
Major-axis diameter, mm/m^2	9.9 ± 1.7	9.7 ± 1.5	10.1 ± 1.8	.333
Minor-axis diameter, mm/m^2	7.7 ± 1.7	7.5 ± 1.6	7.9 ± 1.8	.477
Ostial morphology	0.79 ± 0.18	0.78 ± 0.15	0.79 ± 0.20	.872
Ostial circumference, mm/m^2	30.1 ± 5.0	29.5 ± 5.3	30.7 ± 4.8	.411
Cross-sectional area, mm^2/m^2	107.7 ± 29.8	104.4 ± 30.0	110.5 ± 30.0	.502
Right inferior PV angle	22.3 ± 9.2	22.3 ± 9.3	22.3 ± 9.2	.997

Results are shown as mean ± standard deviation, median [interquartile range], or n (%).
ABL = ablation; LA = left atrium; PV = pulmonary vein; RA = right atrium.

mm/m^2, $P = .9$) (Table 3).[4] Although the duration of radiofrequency ablation time for the right-sided PVs was longer in the Carina-ABL group than in the Non-Carina-ABL group, that for the first-pass applications in the circumferential ablation line was similar between the groups (27.8 ± 6.5 minutes vs 20.5 ± 6.8 minutes, $P = .001$, and 17.8 ± 2.2 minutes vs 17.5 ± 4.3 minutes, $P = .819$, respectively) (Table 3).

Anatomical characteristics

There was no difference in the LA volume index and RA volume index between the Carina-ABL and Non-Carina-ABL groups (35.5 ± 18.7 mL/m^2 vs 39.9 ± 29.1 mL/m^2, $P = .562$, and 29.7 ± 12.0 mL/m^2 vs 32.5 ± 11.3 mL/m^2, $P = .433$, respectively) (Table 2). Also, the LA volume / RA volume ratio did not differ between the groups (0.89 ± 0.24 vs 0.94 ± 0.29, $P = .575$). The PV diameters, PV morphologies, and RIPV angle were all similar between the 2 groups (Table 2). Of note, the interatrial distance in the posterior aspect was significantly shorter in the Carina-ABL group than in the Non-Carina-ABL group, both in the raw data (mm) and in the indexed data (mm/m^2) (13.9 ± 3.0 mm vs 16.8 ± 3.8 mm; $P = .009$, and 7.7 ± 1.7 mm/m^2 vs 9.5 ± 2.3 mm/m^2, $P = .005$, respectively) (Figure 2B). Also, the univariate logistic regression analysis revealed that only the interatrial distance was associated with the necessity of carina ablation (odds ratio, 0.63; 95% confidence interval, 0.45–0.90; $P = .011$) (Figure 3). A representative case with a short interatrial distance in the Carina-ABL group and another with a long interatrial distance in the Non-Carina-ABL group are presented in Figure 4. Similarly, the interatrial distance was significantly shorter in patients with carina breakthrough than those with Bachmann bundle

Table 3 Procedural parameters for right-sided pulmonary vein isolation

	Total (n = 45)	Carina ABL (n = 21)	Non-Carina ABL (n = 24)	*P*
Total procedure time, min	197 ± 38	216 ± 35	180 ± 33	.001
Total mapping points in LA	1479 [1059, 1762]	1596 [988, 1821]	1343 [1143, 1750]	.647
Total mapping points in RA	642 [487, 847]	722 [535, 896]	627 [423, 787]	.307
Bachmann bundle breakthrough	45 (100%)	21 (100%)	24 (100%)	-
Right-sided PV ablation				
Total RF time for RtPV isolation, min	22.3 [17.9, 29.9]	28.5 [23.2, 30.9]	18.1 [16.6, 21.6]	<.001
RF time for 1 round of RtPVs (first-pass applications), min	17.5 [15.8, 18.8]	17.8 [16.1, 19.2]	17.2 [15.5, 18.4]	.391
Total of ablation index values for 1 round of RtPVs	15975 ± 3423	16014 ± 2726	15936 ± 4017	.942
Circumference of RtPV ablation line, mm/m^2	67.3 ± 10.1	67.1 ± 9.3	67.4 ± 11.2	.904
RtPV isolation area, mm^2/m^2	438.2 ± 117.6	422.8 ± 104.3	451.7 ± 128.8	.418
Distance from anterior carina to anterior line for RtPV isolation, mm	8.8 ± 2.2	8.8 ± 2.0	8.8 ± 2.3	.926
Indexed distance from anterior carina to anterior line for RtPV isolation, mm/m^2	4.9 ± 1.2	4.8 ± 1.2	5.0 ± 1.3	.705

ABL = ablation; LA = left atrium; PV = pulmonary vein; RA = right atrium; RF = radiofrequency; RtPV = right-sided PV.

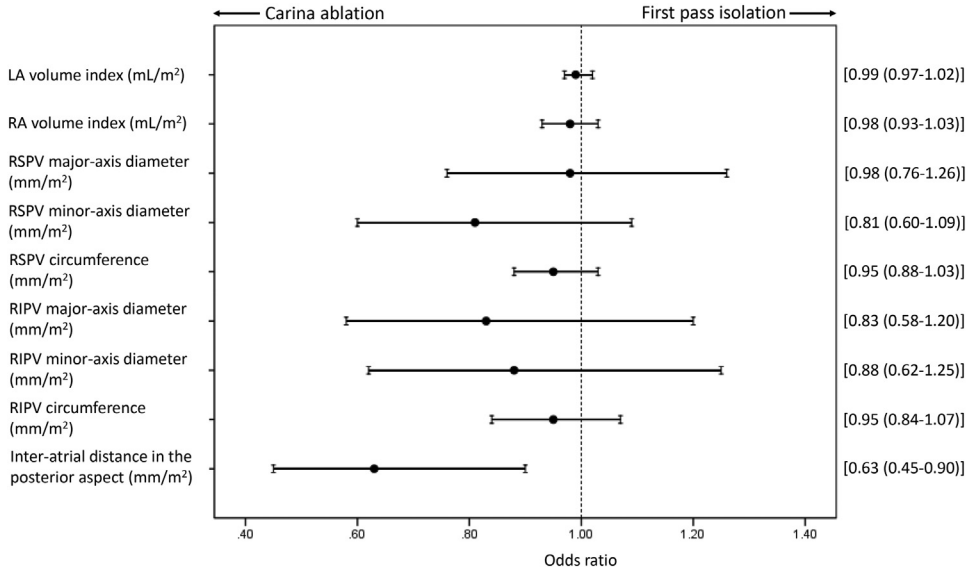

Figure 3 Univariate logistic regression analysis of the measurements on computed tomography imaging. LA = left atrium; RA= right atrium; RIPV= right inferior pulmonary vein; RSPV = right superior PV.

breakthrough alone (7.9 ± 2.1 mm/m^2 vs 9.4 ± 2.2 mm/m^2, P = .024). The sensitivity and specificity and positive and negative predictive values for the necessity of carina ablation at different cut-off values (25th, 50th, and 75th percentile) are shown in Table 4. These values indicated that carina ablation is not necessary to isolate the right-sided PVs in approximately 80% of the patients in whom the interatrial distance is >10 mm/m^2 (75th percentile).

Interobserver variability had an acceptable degree of reproducibility, as reflected by a correlation coefficient of 0.94 for the interatrial distance in the posterior aspect between the 2 investigators. Also, intraobserver variability

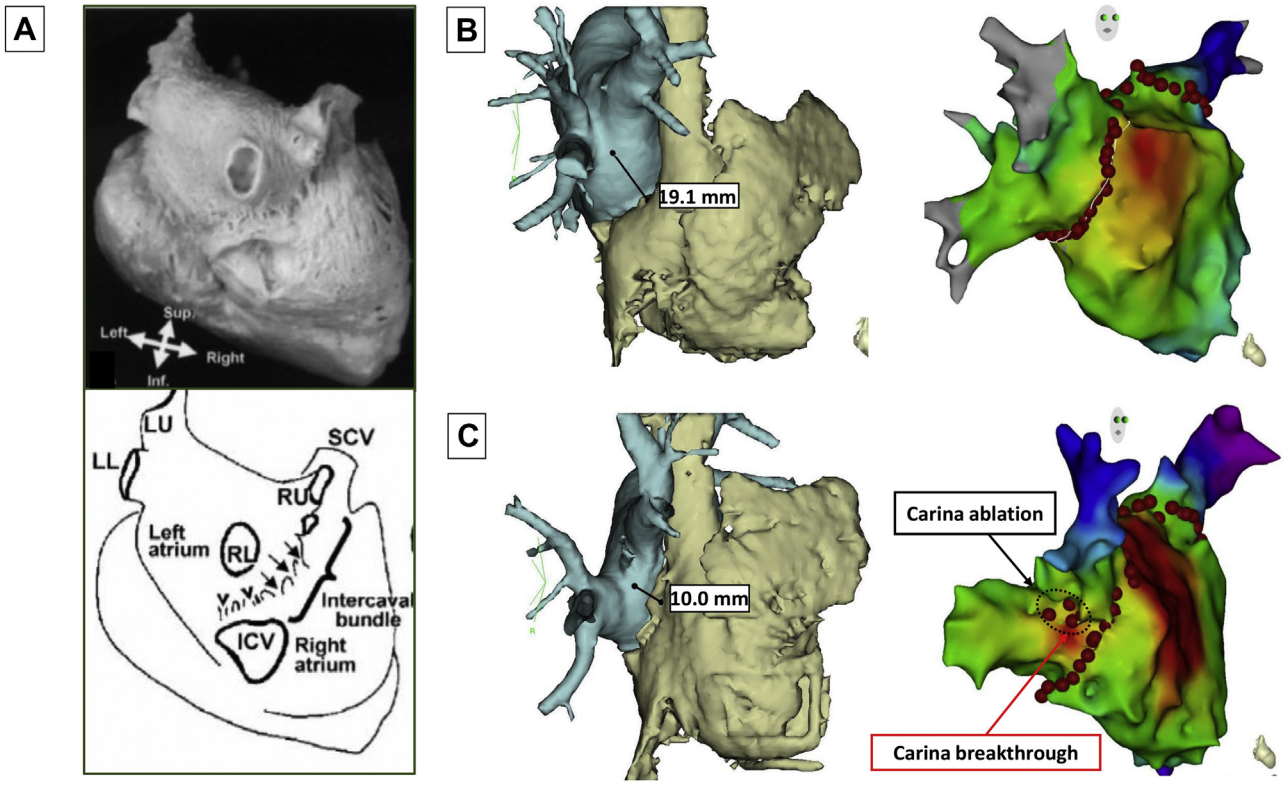

Figure 4 Representative cases. **A:** Histological presentation of epicardial bridging fibers connecting the right and left atria. **B:** A case with long interatrial distance (19.1 mm) in the Non-Carina-ABL group. **C:** A case with short interatrial distance (10.0 mm) in the Carina-ABL group. Corresponding propagation maps are presented in the supplementary video files. ABL = ablation; ICV = inferior caval vein; LL = left lower; LU = left upper; RL = right lower; RU = right upper; SCV = superior caval vein.

Table 4 Sensitivity, specificity, and positive and negative predictive values for the necessity of carina ablation (right-sided pulmonary vein isolation)

	Sensitivity	Specificity	PPV	NPV
RtPV carina breakthrough	90.5%	83.3%	82.6%	90.9%
Cut-off values for interatrial distance				
<6.9 mm/m^2 (25th percentile)	38.1%	91.7%	72.7%	64.7%
<8.5 mm/m^2 (50th percentile)	66.7%	66.7%	63.6%	69.6%
<10.1 mm/m^2 (75th percentile)	90.5%	41.7%	57.6%	83.3%

NPV = negative predictive value; PPV = positive predictive value; RtPV = right-sided pulmonary vein.

had a strong degree of reproducibility, as reflected by a correlation coefficient of 0.97.

Left-sided PV isolation

Patients were also classified into the Carina-ABL group (n = 13) and Non-Carina-ABL group (n = 32) based on the necessity of left-sided PV carina ablation (Supplemental Table 1). In the Carina-ABL group, ablation of high-frequency potentials inside and apart from the posterior ablation line was needed to isolate the veins in 4 (9%) patients. All CT measurement data are presented in Table 5, from which the data of 2 patients with a left common trunk were excluded from the analyses. The short-axis diameter, circumference, and cross-sectional area of the left superior PV were greater in the Non-Carina-ABL group than in the Carina-ABL group (8.6 ± 2.1 mm/m^2 vs 7.3 ± 1.5 mm/m^2, P = .044; 34.9 ± 6.0 mm/m^2 vs 30.1 ± 5.1 mm/m^2, P = .017; and 140.2 ± 45.7 mm^3/m^2 vs 111.9 ± 30.2 mm^3/m^2, P = .048; respectively). Procedure-related data are presented in Supplemental Table 2.

Discussion

Main findings

The key observations of the present study are as follows: (1) In this prospective analysis of LA mapping during sinus rhythm, half of the patients had carina breakthrough in the LA during sinus rhythm mapping. (2) The presence of carina breakthrough before ablation highly predicted the necessity of right-sided PV carina ablation in addition to circumferential ablation encircling the PVs (positive predictive value = 82.6%). (3) Among anatomical variables that can be measured by cardiac CT imaging, only shorter distance between the anterior portion of the carina and RA was a predictor for the necessity of right-sided PV carina ablation. (4) For left-sided PVI, a smaller PV ostium was associated with the necessity of left-sided PV carina ablation.

These results further supported the presence of an epicardial connection between the right-sided PV carina and RA that cannot be eliminated by circumferential ablation.[3–5,7,8] Furthermore, a terminal of the epicardial bridging fiber connecting the LA and RA in the posterior aspect may be more likely to attach inside the circumferential ablation line (ie, the PV carina) when the interatrial distance is shorter.

Anatomy and electrophysiology associated with interatrial epicardial connections

The most prominent interatrial bridge is the Bachmann bundle. In the 1900s, an anatomical study investigated the form and nature of the muscular connection between the primary divisions of the vertebrate heart, including the division between the LA and venous sinus (intercaval bundle). Muscular continuity between the atria is frequently found as bridges in the subepicardium. Bridges joining the LA to

Table 5 Computed tomography measurements (left-sided pulmonary vein isolation)

	Total (n = 43)	Carina ABL (n = 13)	Non-Carina ABL (n = 30)	P
LA volume index, mL/m^2	38.1 ± 24.9	33.6 ± 22.6	40.1 ± 26.1	.439
RA volume index, mL/m^2	31.4 ± 11.7	28.4 ± 14.0	32.9 ± 10.5	.257
LA/RA ratio	0.92 ± 0.27	0.92 ± 0.35	0.92 ± 0.23	.948
Interatrial distance, mm/ m^2	8.6 ± 2.3	8.2 ± 1.6	8.8 ± 2.5	.422
Left superior PV anatomy				
Major-axis diameter, mm/m^2	11.3 ± 2.0	10.6 ± 1.9	11.6± 2.0	.131
Minor-axis diameter, mm/m^2	8.2 ± 2.0	7.3 ± 1.5	8.6 ± 2.1	.044
Ostial morphology	0.74 ± 0.15	0.70 ± 0.15	0.75 ± 0.16	.367
Ostial circumference, mm/m^2	33.5 ± 6.1	30.1 ± 5.1	34.9 ± 6.0	.017
Cross-sectional area, mm^2/m^2	131.7 ± 43.3	111.9 ± 30.2	140.2 ± 45.7	.048
Left inferior PV anatomy				
Major-axis diameter, mm/m^2	9.6 ± 1.3	9.1 ± 1.2	9.7 ± 1.3	.169
Minor-axis diameter, mm/m^2	6.3 ± 1.7	5.9 ± 1.5	6.5 ± 1.7	.302
Ostial morphology	0.66 ± 0.13	0.64 ± 0.13	0.66 ± 0.13	.646
Ostial circumference, mm/m^2	27.1 ± 5.9	26.8 ± 4.1	27.2 ± 6.5	.853
Cross-sectional area, mm^2/m^2	86.1 ± 29.5	78.4 ± 22.7	89.4 ± 31.7	.266

Results are shown as mean ± standard deviation, median [interquartile range], or n (%).
ABL = ablation; LA = left atrium; PV = pulmonary vein; RA = right atrium.

the intercaval area on the RA were clearly presented by an anatomical study[6] (Figure 4A) and can be a site of carina breakthrough of the sinus impulse. Acquired changes in these bridges, which could abolish or prolong interatrial conduction, may provide a substrate for AF. In the late 1990s, catheter ablation aiming at PVI as a treatment for AF was developed and standardized. Because these bridges of muscular continuity connecting the PV carinal region and the RA could preclude PVI by even linear and continuous endocardial lesion sets encircling the ipsilateral PVs, LA and PV anatomy and interatrial connection were revisited.[16] Moreover, in the 2000s, several studies clearly revealed that PVI performed with a wide antral approach, with its longer procedure and ablation times, is more effective than ostial PVI in achieving freedom from total atrial tachyarrhythmia recurrence at long-term follow-up.[17] This approach allowed a terminal of the epicardial bridging fiber to be inside the ablation line encircling the right-sided PVs and required additional radiofrequency applications at that region to achieve PVI. Interestingly, this notion was quantitatively investigated in 2011 by Lin and colleagues,[4] who found that additional carina ablation was likely to be required to obtain right-sided PVI when the distance of the isolation lesions was >8 mm from the PV ostia. The authors suggested epicardial connection within the isolation line as 1 of the mechanisms in their discussion. Patel and colleagues[3] electrophysiologically provided direct proof of the existence of an epicardial connection between the right-sided PV carina and RA by demonstrating electrical isolation of right-sided PVs achieved by ablation at the RA posterior wall where the earliest activation was observed during pacing from inside the PVs. Of note, their ablation strategy was characterized by wider antral isolation, as shown in their 3-D maps.

The interatrial muscular fibers were previously shown by several anatomical studies. In all studies, they lay over the interatrial groove or septal raphe, and were fine and short. It is possible that the closer the LA and RA are in the posterior aspect, the more inside the PV ostia (ie, the PV carina) the attachment of the bridging fiber is. This can be associated with the occurrence of LA breakthrough of the sinus impulse at the carina and the necessity of performing carina ablation for right-sided PVI.

Epicardial connections involving the left-sided PVs

The main reason for the necessity of left-sided PV carina ablation was considered to be involvement of the Marshall bundle in the PV carina region, although multiple variants in the subendocardial and subepicardial fibers around the left-sided PVs were described in an autopsy study.[6] Although the mechanisms behind the larger PV ostium in the Non-Carina-ABL group are unclear, we speculated the following scenario. PV dilation may be a consequence of structural remodeling associated with PV stretch due to left ventricular diastolic dysfunction and inflammation due to persistence of AF and epicardial adipose tissue.[11,18] These factors and the resulting fibrosis could directly and indirectly affect epicardial fibers and the LA and PV sleeve. In the remodeled and dilated PVs, conduction through the Marshall bundle could be pathologically diminished, and initial ablation lesion sets encircling the PVs could be more likely to abolish the Marshall bundle conduction than in the less remodeled and smaller PVs.[8]

Clinical relevance

Theoretically speaking from the endocardial point of view, 1 round of PV ablation with continuous lesion formation achieves PVI, and therefore, operators may be eager to locate conduction gaps and to isolate the veins without performing ablation inside the ablation line. However, this potentially results in excessive formation of ablation lesions that can lead to cardiac tamponade and other collateral damage if an epicardial connection is present. Further, the performance of indiscriminate carina ablation may just increase the risk for PV stenosis. If we preprocedurally estimate an epicardial connection involving the PVs, we could potentially avoid additional futile ablations targeting nonexistent gaps after 1 round of PV ablation.

Currently, the only available method to estimate the presence of an epicardial connection before ablation is activation mapping of the LA during sinus rhythm. The presence of carina breakthrough highly predicted that of a right-sided epicardial connection in the previous and present studies.[5,7,8] However, activation mapping is possible only during sinus rhythm and may require both cardioversion before mapping in patients with AF and the appropriate exclusion of far-field electrograms from the SVC and RA, which are both time-consuming procedures. In contrast, measurements of the interatrial distance on cardiac CT imaging are easy, reproducible, and time-saving and can be noninvasively performed before the ablation procedure. Although the positive predictive value for predicting epicardial connection was higher for the activation mapping method than for the distance measurement method, these advantages may encourage electrophysiologists to measure the interatrial distance before catheter ablation.

One additional important finding was that high-frequency potentials were commonly observed in the successful ablation sites achieving isolation for the carinas on both sides in the present study and in 2 prior case reports.[7,8] If CT measurements predict the necessity of carina ablation, and 1-round ablation does not achieve PVI, this may be a reasonable and efficient way for operators to seek and target high-frequency potentials around the carina region.

Study limitations

First, the study volume was small. A validation cohort may be warranted to evaluate the clinical value of this novel finding. However, this study was prospectively conducted, and therefore, the operator was blinded to the presence or absence of carina breakthrough and the interatrial distance. Second, only patients in whom stable sinus rhythm was maintained during LA mapping were included in this study. The effect of structural changes associated with advanced remodeling due to long-standing persistent AF on the epicardial connection remains to be evaluated. Finally, this

study was primarily designed to investigate epicardial connections involving the right-sided PVs, and therefore, the mechanisms behind the necessity of carina ablation for left-sided PVI were not adequately explored. Further investigation specific to and focusing on the left-sided epicardial connections is needed to clarify this entity.

Conclusions

A shorter interatrial distance for right-sided PVI and a smaller PV ostium for left-sided PVI were associated with the necessity of additional carina ablation. The presence and location of the epicardial fibers may be affected by the atrial and PV geometry.

Funding Sources

This research did not receive any specific grant from funding agencies in the public, commercial, or not-for-profit sectors.

Disclosures

Dr Nogami has received honoraria from Johnson and Johnson and Boehringer-Ingelheim and an endowment from Medtronic Japan and DVx. The other authors declare no conflicts of interest associated with this manuscript.

Appendix

Supplementary data

Supplementary data associated with this article can be found in the online version at https://doi.org/10.1016/j.hroo.2020.08.003.

References

1. Calkins H, Hindricks G, Cappato R, et al. 2017 HRS/EHRA/ECAS/APHRS/SOLAECE expert consensus statement on catheter and surgical ablation of atrial fibrillation. Heart Rhythm 2017;14:e275–e444.
2. Hussein A, Das M, Riva S, et al. Use of ablation index-guided ablation results in high rates of durable pulmonary vein isolation and freedom from arrhythmia in persistent atrial fibrillation patients. Circ Arrhythm Electrophysiol 2018;11:e006576.
3. Patel PJ, D'Souza B, Saha P, Chik WW, Riley MP, Garcia FC. Electroanatomic mapping of the intercaval bundle in atrial fibrillation. Circ Arrhythm Electrophysiol 2014;7:1262–1267.
4. Lin YJ, Tsao HM, Chang SL, et al. The distance between the vein and lesions predicts the requirement of carina ablation in circumferential pulmonary vein isolation. Europace 2011;13:376–382.
5. Yoshida K, Baba M, Shinoda Y, et al. Epicardial connection between the right-sided pulmonary venous carina and the right atrium in patients with atrial fibrillation: A possible mechanism for preclusion of pulmonary vein isolation without carina ablation. Heart Rhythm 2019;16:671–678.
6. Ho SY, Anderson RH, Sánchez-Quintana D. Atrial structure and fibres: morphologic bases of atrial conduction. Cardiovasc Res 2002;54:325–336.
7. Hanaki Y, Hasebe H, Baba M, Yoshida K. Right atrial parasystole originating from isolated activities in the right inferior pulmonary vein with an epicardial connection. HeartRhythm Case Rep 2020;6:437–440.
8. Hasebe H, Furuyashiki Y, Yoshida K. Temporal elimination of an inter-atrial epicardial connection by ablation encircling the right-sided pulmonary veins. HeartRhythm Case Rep, https://doi.org/10.1016/j.hrcr.2020.08.006.
9. Maille B, Das M, Hussein A, et al. Accuracy of left atrial bipolar voltages obtained by ConfiDENSE multielectrode mapping in patients with persistent atrial fibrillation. J Cardiovasc Electrophysiol 2018;29:881–888.
10. Rheinheimer S, Reh C, Figiel J, Mahnken AH. Assessment of right atrium volume by conventional CT or MR techniques: Which modality resembles in vivo reality? Eur J Radiol 2016;85:1040–1044.
11. Yoshida K, Hasebe H, Tsumagari Y, et al. Comparison of pulmonary venous and left atrial remodeling in patients with atrial fibrillation with hypertrophic cardiomyopathy versus with hypertensive heart disease. Am J Cardiol 2017;119:1262–1268.
12. Kistler PM, Earley MJ, Harris S, et al. Validation of three-dimensional cardiac image integration: use of integrated CT image into electroanatomic mapping system to perform catheter ablation of atrial fibrillation. J Cardiovasc Electrophysiol 2006;17:341–348.
13. Kim YH, Marom EM, Herndon JE 2nd, McAdams HP. Pulmonary vein diameter, cross-sectional area, and shape: CT analysis. Radiology 2005;235:43–49. discussion 49–50.
14. Tsyganov A, Petru J, Skoda J, et al. Anatomical predictors for successful pulmonary vein isolation using balloon-based technologies in atrial fibrillation. J Interv Card Electrophysiol 2015;44:265–271.
15. Kaneshiro T, Matsumoto Y, Nodera M, et al. Anatomical predisposing factors of transmural thermal injury after pulmonary vein isolation. Europace 2018;20:1122–1128.
16. Ho SY, Cabrera JA, Sanchez-Quintana D. Left atrial anatomy revisited. Circ Arrhythm Electrophysiol 2012;5:220–228.
17. Proietti R, Santangeli P, Di Biase L, et al. Comparative effectiveness of wide antral versus ostial pulmonary vein isolation: a systematic review and meta-analysis. Circ Arrhythm Electrophysiol 2014;7:39–45.
18. Hasebe H, Yoshida K, Iida M, et al. Differences in the structural characteristics and distribution of epicardial adipose tissue between left and right atrial fibrillation. Europace 2018;20:435–442.